OPERATION OF HIGH-POWER 8.6 AND 17.1 GHz COAXIAL GYROKLYSTRONS*

W. Lawson, B. Hogan, M. Castle, V. L. Granatstein, M. Reiser, X. Xu
Institute for Plasma Research, University of Maryland, College Park, MD 20742

Abstract

At the University of Maryland, we have designed, constructed, and tested a number of gyroklystron tubes operating from X-Band to Ka-Band over the past several years [1]. The purpose of this effort is to examine the suitability of gyro-amplifiers as drivers for advanced accelerator applications such as the Next Linear Collider. We are currently conducting a series of experiments with coaxial tubes which are designed to produce peak powers in excess of 100 MW in X- and Ku-Band, increasing the state-of-the-art by a factor of 3-5. Preliminary results have indicated peak powers in excess of 75 MW at 8.6 GHz in a three cavity first-harmonic gyroklystron tube with a gain near 30 dB and an efficiency near 32%. In this paper we will detail the experimental results of this tube and discuss designs and preliminary cold test results of a 3-cavity second-harmonic device, which is expected to give comparable results at 17.14 GHz.

1 INTRODUCTION

At the University of Maryland, we have been investigating the suitability of high power gyro-amplifiers as drivers for linear colliders for over a decade. [1] To this end, we have designed, constructed, and tested a variety of gyroklystron and gyrotwystron tubes operating from X-Band to Ka-Band. With a 440 kV, 160-260 A beam, we were able to produce about 30 MW of peak power in 1 μs pulses near 9.87 and 19.7 GHz with first- and second-harmonic gyroklystron tubes, respectively. The peak efficiencies were near 30% and the large-signal gains were 25-35 dB. Circular electric modes were used in all cavities and the average beam velocity ratio was always near one. Efficiency was limited by instabilities in the beam tunnel preceding the input cavity and beam power was limited by the electron gun.

The focus in the past few years has been to upgrade the system to achieve peak powers approaching 100 MW in X- and Ku-Band. The increase in power results from a larger beam current, which is achieved by maintaining the same current density, but enlarging the average beam radius. Subsequently, the tube cross-sectional dimensions are increased and an inner conductor is required to maintain cutoff to the operating mode in the drift regions. To date, we have hot-tested a 2-cavity and a 3-cavity first harmonic tube and we are about to test a 3-cavity second harmonic tube.

In this paper we first discuss the experimental test facility. Then we discuss the computer simulations before describing the experimental results from our X-Band tubes. Finally, we mention our Ku-Band progress before closing with our near and long term goals.

2 EXPERIMENTAL TEST FACILITY

The voltage pulse is generated with a line-type modulator which is capable of producing 2 μs flat-top pulses at up to 2 Hz with voltages and currents up to 500 kV and 800 A, respectively. A capacitive voltage divider and a current transformer are used to measure the time evolution of the voltage and current. Our single-anode MIG is

Table I. The system parameters.

Beam parameters	
Beam Voltage (kV)	470
Beam Current (A)	505
Average Velocity Ratio	1.05
Axial velocity spread (%)	4.4
Magnetic field parameters	
Input cavity field (kG)	5.69
Buncher cavity field (kG)	5.38
Output cavity field (kG)	4.99
Input and buncher cavity parameters	
Inner radius (cm)	1.10
Outer radius (cm)	3.33
Length (cm)	2.29
Quality factor	70 ± 15
Output cavity parameters	
Inner radius (cm)	1.01
Outer radius (cm)	3.59
Length (cm)	1.70
Quality factor	135 ± 10
Drift tube parameters	
Inner radius (cm)	1.83
Outer radius (cm)	3.33
Length (between I-B) (cm)	5.18
Length (between B-O) (cm)	5.82
Amplifier Results	
Drive Frequency (GHz)	8.60
Output power (MW)	75
Pulse length (μs)	1.7
Gain (dB)	29.7
Efficiency (%)	31.5

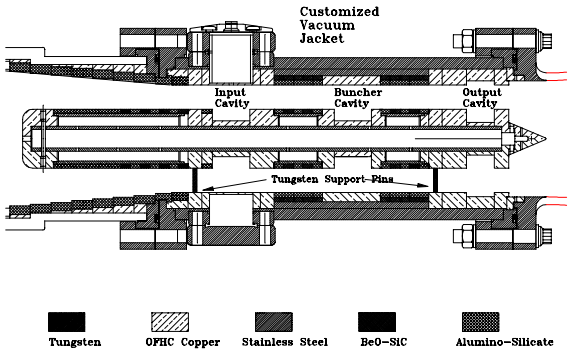

Figure 1. The three-cavity microwave circuit.

capable of producing a 500 kV, 720 A beam with an average orbital-to-axial velocity ratio of $\alpha = 1.5$ and an axial velocity spread of $\Delta v_z/v_z < 10\%$. The beam parameters are given in Table I for the operating point where maximum amplification occurs. The voltage and current are measured quantities; all other values come from the EGUN simulations and are based on the MIG geometry and the magnetic field profile. The actual theoretical fields at the centers of the three cavities are given in Table I. The axial field is detuned by -3.5% in the input cavity, -8.8% in the buncher cavity and -15.4% in the output cavity.

The 3-cavity microwave circuit is shown in Fig. 1 and the key dimensions are given in Table I. The inner conductor is supported by two thin tungsten pins and forces the drift tubes to be cutoff to the TE_{01} mode at 8.6 GHz. The inner conductor only extends a few centimeters into the downtaper and is rapidly terminated after the output cavity. Lossy ceramics are placed in the drift regions to suppress spurious modes. The rings on the inner conductor generally alternate between carbon-impregnated alumino-silicate (CIAS) and 80% BeO-20% SiC. Two layers of lossy ceramics are placed along the outer conductor in the drift regions. The outer layer is BeO-SiC and the inner layer is CIAS. The 2-cavity circuit omits the buncher cavity and has a longer drift region.

The input cavity is defined by a decrease in the inner conductor radius. The cavity loss is roughly evenly divided between the coupling aperture and a CIAS ring on the inner conductor which is placed adjacent to the cavity. The power to the input cavity is supplied by a 150 kW coaxial magnetron. The buncher cavity has identical dimensions for the metal components. However, the Q is determined entirely by CIAS ceramics.

The output cavity is defined by radial changes on both walls and the lip radii are equal to the drift tube radii. The quality factor is dominated by the diffractive Q which is adjusted by changing the length of the coupling lip.

3 THEORETICAL AND EXPERIMENTAL RESULTS

3.1 First-Harmonic Results

A partially self-consistent large-signal code is used to design the circuit and magnetic field configuration and to estimate the performance of the tube at the actual operating point. A small-signal start-oscillation code is used to determine the stability properties of the cavities and set limits on the cavity quality factors. The solid line in Fig. 2 shows the expected performance of the tube as a function of velocity spread for α=1.5. The simulation predicts a zero-spread efficiency of 43%, and an efficiency of 34% for 10% spread. For the 6% spread predicted for a 500 A beam, the simulated interaction efficiency is about 40%. All microwave cavities are expected to be stable at the design operating point for the quality factors indicated in Table I. The theoretical efficiency for the 2-cavity tube is slightly less, but the predicted gain is significantly lower. Consequently, the 2-cavity tube was gain-limited and produced less than 1 MW of output power.

The optimal parameters and experimental results have been listed in Table I. The values are all taken from anechoic chamber measurements. The time dependence of

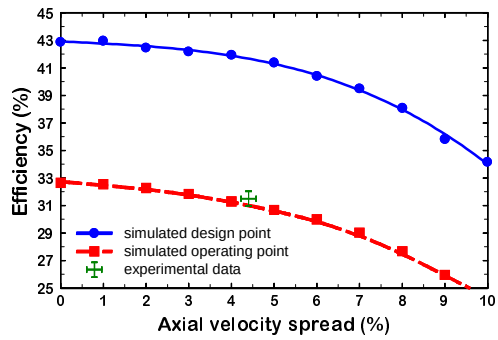

Figure 2. Efficiency versus velocity spread.

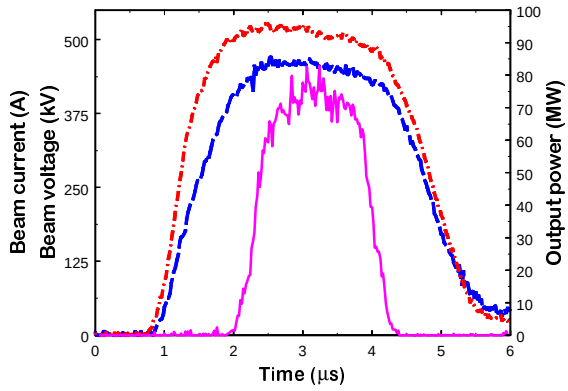

Figure 3. Time dependence of the output pulse.

the beam voltage (dashed line), beam current (dot-dashed line), and the amplified signal (solid line) are shown in Fig. 3. There is a slight droop on the flat top due to mismatches in the modulator. The peak values indicated in Table I represent the average value of the signal in the flat top region. The peak power is about 75 MW, which represents an efficiency of nearly 32%. The corresponding gain is almost 30 dB and the pulse width is 1.7 μs (FWHM). Attempts to increase the peak power further by raising the beam's velocity ratio result in a sharp cut in the output signal near the maximum value which is usually indicative of an instability (though none were detected by the microwave diagnostics).

An EGUN simulation using the parameters of the operating point indicate that the beam's velocity ratio at the entrance to the circuit is near one. There is a reasonably large uncertainty in this ratio due to the neglect of the self-axial magnetic field in EGUN and the uncertainty in the applied field at the cathode. In a previous experiment at the University of Maryland, for example, the measured average velocity ratio was consistently higher than the simulated ratio by about 15%. [2] Simulations of the amplifier performance at the operating point are given by the dashed line in Fig. 2. The simulated cathode magnetic field is adjusted slightly to produce the best match between the theoretical efficiency and the measured efficiency, which is indicated by the cross. The required field is about 20 G lower than the calculated ideal field and well within the uncertainties of the experimental data.

3.2 Second Harmonic Tube

The second harmonic tube is realized by keeping the first harmonic tube's input cavity but replacing the buncher and output cavities with ones that resonate at twice the drive frequency in the TE_{021} mode. Such cavities

Table II. The second harmonic design.

Beam voltage (kV)	500
Beam current (A)	770
Velocity ratio	1.51
Input cavity Q	50
Buncher cavity Q	389
Output cavity Q	320
Gain (dB)	49
Efficiency (%)	41
Output power (MW)	158

are normally difficult to realize, because the cavity's end walls generate other radial modes due to the beam tunnel opening. For cavity isolation, the fields must not leak substantially into the drift regions, yet the operating frequency is well above the cutoff of the TE_{01} mode. In circular waveguide systems, the usual way to avoid this problem is to introduce smoothly-varying wall radii, but the added length of these transitions is usually unacceptable. Fortunately, in coaxial tubes, making the radial wall transitions that define the TE_{021} cavity approximately

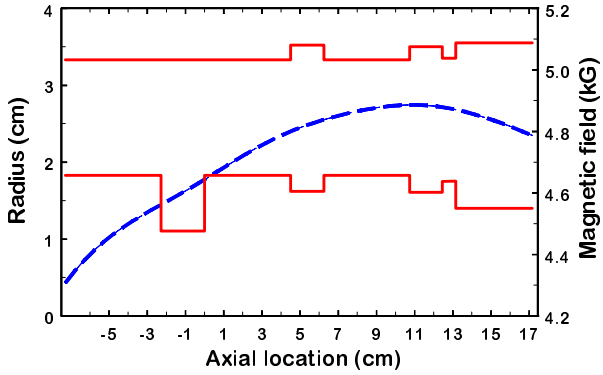

Figure 4. The shape of the second harmonic tube and the simulated optimal magnetic field profile (dashed line).

equal on the inner and outer walls naturally leads to a mode with very little conversion to the TE_{01} modes and subsequent leakage fields.

The principal design parameters for our three cavity second harmonic tube are given in Table II along with the simulated performance estimates. The cavity profile is shown in Fig. 4. The overall length is very similar to the first harmonic tube. At this point, the tube components have been constructed, the cavities have been adjusted to achieve the required frequencies and quality factors, and the tube is installed in our test facility. Hot testing should commence in the next few days.

4 SUMMARY

In summary, we have developed an X-band coaxial gyroklystron which has increased the state-of-the-art in peak power for gyroklystrons by nearly a factor of 3. In the near future we will test our 2nd harmonic tube, with the goal of obtaining about 100-150 MW of peak power at 17.136 GHz. We will investigate the limitations on velocity ratio in greater detail and attempt to increase the nominal velocity ratio to the original design value. In the long term we expect to build and power a 17.136 GHz accelerator structure with an accelerating gradient near 200 MV/m.

5 ACKNOWLEDGEMENTS

The authors would like to thank N. Ballew, P. Chin, J. Cheng, P. E. Latham, G. Nusinovich, and G. P. Saraph for their contributions to this work.

6 REFERENCES

[1] V. L. Granatstein and W. Lawson, "Gyro-Amplifiers as Candidate RF Drivers for TeV Linear Colliders," IEEE Trans. on Plasma Science, Vol. 24, pp. 648-665 (1996).

[2] J. P. Calame and W. Lawson, *IEEE Trans. Electron Devices*, vol. 38, p. 1538 (1991).